

CrystEngComm

Accepted Manuscript



This is an *Accepted Manuscript*, which has been through the Royal Society of Chemistry peer review process and has been accepted for publication.

Accepted Manuscripts are published online shortly after acceptance, before technical editing, formatting and proof reading. Using this free service, authors can make their results available to the community, in citable form, before we publish the edited article. We will replace this *Accepted Manuscript* with the edited and formatted *Advance Article* as soon as it is available.

You can find more information about *Accepted Manuscripts* in the [Information for Authors](#).

Please note that technical editing may introduce minor changes to the text and/or graphics, which may alter content. The journal's standard [Terms & Conditions](#) and the [Ethical guidelines](#) still apply. In no event shall the Royal Society of Chemistry be held responsible for any errors or omissions in this *Accepted Manuscript* or any consequences arising from the use of any information it contains.

Coordination Polymers Based on Copper Carboxylates and Angular 2,5-bis(imidazol-1-yl)thiophene (thim₂) Ligand: Sequential Structural Transformations

Namita Singh^a, Pratap Vishnoi^b and Ganapathi Anantharaman^{*a}

^a*Department of Chemistry, Indian Institute of Technology (IIT), Kanpur – 208016, India.*

^b*Department of Chemistry, Indian Institute of Technology (IIT), Bombay, Powai, Mumbai – 400076, India.*

Email: garaman@iitk.ac.in.

Abstract

Four CPs [Cu(thim₂)(OOCCH₃)₂]_n (**1**), [Cu₂(thim₂)(μ₂-OOCCH₃)₄]_n (**2**), [Cu₂(thim₂)₂(μ₂-OOCCH₃)₂(OOCCH₃)₂]_n (**3**) and {[Cu₂(thim₂)₂(μ₂-OH₂)(OOCCH₃)₄]}·4H₂O (**4**) have been synthesized and characterized. 1D helical CP (**1**) was formed by using copper acetate and 2,5-bis(imidazol-1-yl)thiophene (thim₂). Whereas, upon addition of two equivalents of benzoic acid resulted in the formation of 1D zig-zag chain (**2**) consisting of paddle wheel copper benzoate unit. Interestingly, CP **2** undergoes one pot sequential SC-SC transformations in A-B-C manner to another kinetically more stable 1D ladder type chain (**3**) in the presence of air and excess ligand in solution before forming a thermodynamically stable 2D network (**4**) in mother solution. The cause for these transformations (**2-4**) and magnetic behavior (**1-3**) of the CPs has been discussed.

Introduction:

Metal carboxylates are of immense interest for designing polymeric architectures of coordination polymers (CPs) or metal organic frameworks (MOFs) due to their higher stability and flexibility, these unique structural features impart potential applications for sorption and catalysis as well as magnetic materials.¹⁻³ CPs of stable and flexible framework are more feasible for structural transformation both in solid and solution. The study of crystal transformations without loss of crystallinity (single crystal to single crystal (SC-SC)) is in current interest and provides the chance to monitor the structural changes in solid state. These are influenced by various factors including solvents and external stimuli such as light and heat which induces the movement of the molecules in the lattice leading to the isolation of different products.⁴⁻⁶ Apart from that relative kinetic and thermodynamic stability can also be an important factor for stimulating the structural transformations.⁷⁻¹² The SC-SC transformation in the MOFs or CPs based on metal carboxylates has been widely studied due to the structural integrity of the host during the reversible sorption of guest molecules.¹³ In contrast the SC-SC transformations with structural changes in the CPs based on multi-nuclear metal carboxylate SBUs is of great interest as they can play an important role in understanding of bond breaking and formation phenomenon.^{4, 5, 14-16} In this regard, dinuclear paddle wheel clusters are well known as building block in CPs because of higher stability and ability to tune the structure by altering the nature of carboxylates and/or ancillary ligands.¹⁷ Recently, there are examples found in CPs which include reversible breaking or formation of paddle wheel unit with occasional change in the metal ion geometry in the corresponding structures.¹⁸⁻²⁰ These changes occasionally cause significant impact on the physical properties, such as sorption and magnetism.^{5, 18}

The particular interest is the structural transformation of MOFs or CPs containing paddle wheel copper carboxylates which have been synthesized using multi-carboxylate linkers and the linear or angular ligands. There are few examples of copper (II) carboxylates containing paddle wheel unit which undergo reversible or irreversible structural transformations in presence of solvent molecules, temperature and air.²¹⁻²⁴ These changes are also witnessed by the changes in physical property such as color. Also, it is known that the paramagnetic copper ion with carboxylate groups generate interesting magnetic materials because carboxylate groups can transfer interactions between copper centers through super exchange pathways.²⁵⁻²⁷ Magnetism for the dinuclear paddle wheel or polynuclear copper carboxylates was studied for long time. Such studies were extended for the CPs to understand the magnetic properties of the resulting CPs or MOFs.^{28, 29} In addition dinuclear copper carboxylate clusters have gained the special attention because of their wide use in pharmaceutical, absorbent and catalyst as well as biological importance.³⁰⁻³⁵

We have been involved in investigating the structural diversity of CPs synthesized from angular tritopic 2,5-bis(imidazol-1-yl)thiophene (thim_2) ligand with various metal sulphates and metal carboxylates containing different multicarboxylic acids as co-ligands.^{36, 37} In continuation, we have synthesized and characterized the four CPs $[\text{Cu}(\text{thim}_2)(\text{OOCCH}_3)_2]_n$ (**1**), $[\text{Cu}_2(\text{thim}_2)(\mu_2\text{-OOC}_6\text{H}_5)_4]_n$ (**2**), $[\text{Cu}_2(\text{thim}_2)_2(\mu_2\text{-OOC}_6\text{H}_5)_2(\text{OOC}_6\text{H}_5)_2]_n$ (**3**) and $\{[\text{Cu}_2(\text{thim}_2)_2(\mu_2\text{-OH}_2)(\text{OOC}_6\text{H}_5)_4] \cdot 4\text{H}_2\text{O}\}$ (**4**) using copper carboxylates (acetates/benzoates) with thim_2 . Interestingly, the green colored crystals of **2** undergo sequential transformation first into blue-colored crystals of 1D ladder type structure (**3**) before forming dark blue crystals of 2D structure (**4**) in SCSC manner. Herein the synthesis, structural characterization, magnetism (**1-3**) and the cause for the transformations (**2-4**) are reported.

Experimental Section

Materials and physical measurements.

2,5 dibromo thiophene, CuI (Sigma Aldrich) as well as other chemicals such as anhyd. K_2CO_3 , imidazole and metal salts (sd fine-CHEM. Ltd.) were obtained and used as received. Solvents were received, from SD Fine-Chem. Ltd. and purified by standard procedures prior to use.³⁸ $Thim_2$ was prepared according to the reported literature procedure.³⁷ Infrared spectra (IR) were recorded using KBr pellet on Perkin–Elmer model 1320 spectrometer in the range of 4000–400 cm^{-1} . Thermogravimetric analysis (TGA) was performed under nitrogen atmosphere (heating rate of 5°C/min) on Mettler Toledo star system. Microanalyses for all the compounds were collected using Perkin Elmer Series-II 2400 Elemental Analyzer. Powder X-ray diffraction spectra (CuK_{α} radiation, scan rate 3°/min, 293 K) were collected on a Bruker D8 advance series 2 Powder X-ray diffractometer. Magnetic measurements were carried out on powdered samples using Quantum Design MPMSXL-7 SQUID magnetometer. Diamagnetic corrections were calculated using Pascal's constant.³⁹

Single-Crystal X-ray Studies

Single crystal X-ray data were recorded on a Bruker SMART APEX CCD diffractometer using graphite-monochromated $Mo-K_{\alpha}$ radiation ($\lambda = 0.71073 \text{ \AA}$) at 100 K (for **1**, **3** and **4**) and 150 K on a Rigaku Saturn 724 CCD diffractometer with a $Mo-K_{\alpha}$ radiation source ($\lambda = 0.71075 \text{ \AA}$) (for **2**). All the structures were solved by the direct method employing SHELXS-97 (for **1**, **3** and **4**) and SIR-92⁴⁰ (for **2**). SHELXL-97⁴¹ (for **1**, **3** and **4**) and SHELX-97⁴² (for **2**) were used to refine on F^2 with full-matrix least squares technique. All hydrogen atoms were fixed in idealized position using a riding model. Non hydrogen atoms were refined anisotropically. The disordered water molecules present in the lattice of CP **4** were treated by squeeze refinement using

PLATON.⁴³ All the squeezed water molecules have been included in the empirical formula as well as formula weight of CP 4. The crystal and refinement data are mentioned in Table 1 while selected bond lengths and angles are depicted in Table S1.

Synthesis of [Cu(thim₂)(OOCCH₃)₂]_n (1). Cu(OOCCH₃)₂·2H₂O (0.03 g, 0.15 mmol) and thim₂ (0.032 g, 0.15 mmol) was dissolved in DMF (3 mL) and methanol was diffused in this solution by slow evaporation. Blue color single crystals were obtained after 4 days. Yield: 0.043 g (based on Cu(OOCCH₃)₂·H₂O, 72.88 %). Anal. Calcd. for C₁₄H₁₄N₄O₄SCu (%): C, 42.25; H, 3.55; N, 14.08 %. Found: C, 42.00; H, 3.65; N, 13.72 %. IR (cm⁻¹) 3500(br), 3139(w), 3099(m), 3051(w), 3006(w), 1575(vs), 1532(m), 1493(s), 1386(vs), 1352(m), 1332(s), 1321(s), 1269(m), 1250(m), 1203(m), 1114(s), 1055(s), 1009(w), 921(w), 791(m), 777(m), 748(m), 680(m), 656(m), 620(m), 555(w), 475(w), 415(w).

Synthesis of [Cu₂(thim₂)(μ₂-OOCCH₃)₄]_n (2). Two synthetic strategies were used for the preparation of compound 2.

Path A. A methanolic solution (3 mL) of thim₂ (0.032 g, 0.15 mmol) was layered on DMF solution (2 mL) of Cu(OOCCH₃)₂·2H₂O (0.03 g, 0.15 mmol) and C₆H₅COOH (0.037 g, 0.3 mmol) in a culture tube and closed tube kept for crystallization. Green color single crystals were obtained after 24 h. Yield: 0.032 g (based on Cu(OOCCH₃)₂·H₂O, 52.45 %). Anal. calcd for C₃₈H₂₈N₄O₈SCu₂ (%): C, 55.13; H, 3.41; N, 6.77 % Found: C, 54.16; H, 3.21; N, 6.84 %. IR (cm⁻¹) 3442(br), 3126(br), 3059(br), 1629(vs), 1572(vs), 1494(m), 1402(vs), 1320(w), 1305(w), 1235(w), 1210(br), 1174(w), 1115(w), 1068(w), 1049(m), 1024(w), 934(w), 843(w), 821(w), 795(w), 719(vs), 684(s), 652(w), 619(w), 549(br), 483(w).

Path B. The same reaction procedure was used as mentioned in Path A except that $\text{Cu}(\text{OOCCH}_3)_2 \cdot \text{H}_2\text{O}$ (0.03 g, 0.15 mmol), $\text{C}_6\text{H}_5\text{COOH}$ (0.037 g, 0.3 mmol) and thim_2 (0.016 g, 0.075 mmol) was used. Green colored single crystals were obtained after 24 h. Yield: 0.039 g (based on $\text{Cu}(\text{OOCCH}_3)_2 \cdot \text{H}_2\text{O}$, 63.93 %).

Synthesis of $[\text{Cu}_2(\text{thim}_2)_2(\mu_2\text{-OOCCH}_6\text{H}_5)_2(\text{OOCCH}_6\text{H}_5)_2]_n$ (3**).** Two synthetic strategies were used for the preparation of **2**.

Path A. Exposure of the mother liquor (Path A of **2**) containing green colored crystals of **2** to air led to the formation of blue colored crystals within 24 h. Yield: 0.043 g (based on $\text{Cu}(\text{OOCCH}_3)_2 \cdot \text{H}_2\text{O}$, 55.12 %). Anal. Calcd for $\text{C}_{24}\text{H}_{18}\text{N}_4\text{O}_4\text{SCu}$ (%): C, 55.21; H, 3.47; N, 10.73 % Found: C, 54.53; H, 3.36, N, 10.53 %. IR (cm^{-1}) 3448(br), 3140(w), 3102(m), 1629(s), 1604(vs), 1570(vs), 1530(m), 1495(s), 1446(w), 1365(vs), 1310(m), 1240(w), 1209(w), 1171(w), 1117(m), 1097(w), 1066(s), 1050(m), 1037(w), 1024(w), 948(m), 921(w), 901(br), 863(br), 837(m), 820(m), 762(vs), 715(m), 674(m), 647(s), 618(w), 554(w), 427(w).

Path B. Thim_2 (0.016 g, 0.075 mmol) was added to the mother solution of **2** containing crystals (path B). The resultant mixture was exposed under air which led to formation of blue colored crystals of **3** within 24 h. Yield: 0.041 g (based on $\text{Cu}(\text{OOCCH}_3)_2 \cdot \text{H}_2\text{O}$, 52.56 %).

Synthesis of $\{[\text{Cu}_2(\text{thim}_2)_2(\mu_2\text{-OH}_2)(\text{OOCCH}_6\text{H}_5)_4] \cdot 4\text{H}_2\text{O}\}_n$ (4**).** The same synthetic procedure as for **3** (Path A) was used except that mother solution of **3** containing blue crystals was exposed to air for prolonged period for about 20 days. The dark blue colored crystals of **4** were obtained.

Results and Discussion

CPS **1-4** were prepared by the reaction of copper acetate with ligand thim_2 in the mixture of DMF/MeOH. The reaction of copper acetate and thim_2 using benzoic acid as co-ligand in

1:1:2 molar ratio afforded green color crystals of $[\text{Cu}_2(\text{thim}_2)(\mu_2\text{-OOCC}_6\text{H}_5)_4]_n$ (**2**) within 24h. When mother solution of CP **2** containing crystals was exposed to the air, green crystals converted into blue crystals of $[\text{Cu}_2(\text{thim}_2)_2(\mu_2\text{-OOCC}_6\text{H}_5)_2(\text{OOCC}_6\text{H}_5)_2]_n$ (**3**) within 24h through SCSC transformation (Figure 3). Further standing on ambient condition for 20 days, blue crystals in solution transform into dark blue crystals of $\{[\text{Cu}_2(\text{thim}_2)_2(\mu_2\text{-OH}_2)(\text{OOCC}_6\text{H}_5)_4] \cdot 4\text{H}_2\text{O}\}_n$ (**4**) in SCSC manner. It is apparent that CP **2** is a kinetic product, while CPs **3** and **4** are kinetically more stable and thermodynamic product respectively. However as shown in path B of scheme 1, use of copper acetate, thim_2 and benzoic acid in 1:0.5:2 molar ratio also afford the CP **2** and crystals were found to be stable in mother solution upon exposure to the air. The addition of solid thim_2 in the mother solution containing crystals of **2** (path B) led to the transformation of green crystals (**2**) to blue crystals (**3**) within 24 h in presence of air which confirms, the presence of excess thim_2 in solution and exposure of the mother solution to air drive the transformation of **2** in **3**. During the overall transformation from **2** to **4** dissolution/recrystallization process were not observed. CPs **1-4** were found to be highly stable after separating from the solution and insoluble in common organic solvents. The infrared spectrum of CPs **1** and **2** displayed $\nu_{\text{as(OCO)}}$ and $\nu_{\text{s(OCO)}}$ vibrations of carboxylate groups at 1573 cm^{-1} and 1386 cm^{-1} for **1** and 1672 cm^{-1} and 1402 cm^{-1} for **2**. The observed $\Delta\nu$ in the complexes suggests monodentate and bridging bidentate coordination modes of carboxylate groups respectively. Also, CP **3** display multiple carboxylate stretching frequencies, $\nu_{\text{as(OCO)}}$ and $\nu_{\text{s(OCO)}}$ for carboxylate groups at $1604(\text{vs})\text{ cm}^{-1}$, $1570(\text{vs})\text{ cm}^{-1}$ and $1495(\text{s})\text{ cm}^{-1}$, $1365(\text{vs})\text{ cm}^{-1}$ respectively which suggest more than one type of coordination modes to the copper ion.^{44,45}

Single-crystal X-ray structure of CPs 1-4

Structural analysis of $[\text{Cu}(\text{thim}_2)(\text{OOCCH}_3)_2]_n$ (**1**)

The reaction of copper acetate with thim_2 in DMF/MeOH medium resulted in blue colour crystals of CP **1** that crystallizes in monoclinic $P2_1/n$ space group. Asymmetric unit contains one Cu(II) ion, one thim_2 ligand and two acetate anions. It consists of a square planar copper(II) ion coordinated by two oxygen atoms from two different acetates ions in monodentate fashion and two imidazole nitrogen atoms from two distinct thim_2 ligands (Figure 1a). The bridging feature of thim_2 through imidazole nitrogen units gives rise to an infinite 1D helical chain (Figure 1a). The average Cu–N and Cu–O distances are 1.988 (4) Å and 1.957(5) Å respectively, which are well within the reported values in the literature.⁴⁶ Due to the C–N bond rotation, two imidazole rings within thim_2 ligand are almost perpendicular to each other with 84.11° dihedral angle. 1D chains form a 3D structure through C–H \cdots O supramolecular interactions (in *bc* plane) and other short contact interactions (along *a* direction) (Figure 1b; S1a-b).

Structural analysis of $[\text{Cu}_2(\text{thim}_2)(\mu_2\text{-OOC}_6\text{H}_5)_4]_n$ (**2**)

Single crystal X-ray diffraction analysis of **2** reveals the formation of paddle wheel units of copper(II) benzoate connected by the imidazole nitrogen atoms of thim_2 at the axial position to form a 1D chain (Figure 2a). Thus the overall composition of metal: thim_2 in **2** is 1:0.5 equivalent. The Cu–O bond distances are varied in the range of 1.958(9) Å–1.994(8) Å which are comparable with the previously reported dimeric unit $[\text{Cu}_2(\text{OOCPh})_4(\text{pyz})]_n$.⁴⁷ The adjacent and diagonal O–Cu–O bond angles are found between the range of 87.7(2)°–90.8(3)° and 167–168° respectively.

The Cu–Cu distances within the paddle wheel units and in the intra-chain connected by the thim_2 are 2.65 Å (av.) and 13.25 Å respectively. In the paddle wheel units, one of the eight

membered $\text{Cu}_2\text{C}_2\text{O}_4$ rings (Cu1O1O2Cu#1O#1O#2 and Cu2O7O8Cu#2O#7O#8) and the phenyl rings bounded to them are in plane whereas other eight membered $\text{Cu}_2\text{C}_2\text{O}_4$ rings and the phenyl rings are not in plane. The planar eight membered rings in the adjacent paddle wheel units are oriented by 70.00° . Consequently, the inter-chain $\text{C-H}\cdots\pi$ interactions between planar and non-planar rings was observed (Figure S2a). These interactions lead to the formation of a supra-molecular network in *bc* plane. This network extend along *a* direction through short contact interactions between imidazole (C1) and (C14, C15 and C16) carbon atoms of phenyl rings and $\text{C-H}\cdots\text{O}$ interactions between the backbone C-H of thiophene (C6–H6), imidazole (C3–H3) groups and the oxygen atoms (O3 and O7) of carboxylate units (Figure S2b). The dihedral angle between the imidazole rings is 82.55° and the larger value could be due to these inter-chain $\text{C-H}\cdots\text{O}$ interactions. Besides, inter-chain planar phenyl rings bound to the planar $\text{Cu}_2\text{C}_2\text{O}_4$ show face to face $\pi\cdots\pi$ and $\text{C-H}\cdots\pi$ interactions (like lock and key) in *ab* plane (Figure S2c). As a result of these interactions, a 3D supra-molecular structure is obtained (Figure 2c). In 3D, distance between two copper centres of adjacent inter-chains (Cu1-Cu#1:10.07 Å along 'a' and Cu1-Cu#1: 10.68 Å 'b' direction respectively) is closer as compared to the intra-chain distances.

Structural analysis of $[\text{Cu}_2(\text{thim}_2)_2(\mu_2\text{-OOC}\text{C}_6\text{H}_5)_2(\text{OOC}\text{C}_6\text{H}_5)_2]_n$ (**3**)

Surprisingly, exposure of the mother solution of **2** containing green crystals (Path A) under air resulted in blue colored crystals of **3** within 24 h (Figure 3). Crystals of CP **2** obtained through path B show stability in solution upon exposure to air and transform to the CP **3** in SC-SC manner on addition of ligand in solution. Single crystal X-ray analysis of **3** shows a 1D ladder type chain structure composed of 1:1 metal-thim₂ ratio. The dimeric paddle wheel $[\text{Cu}_2(\text{OOC}\text{C}_6\text{H}_5)_4]$ unit of **2** breaks to form a new dimeric unit $[\text{Cu}_2(\text{OOC}\text{C}_6\text{H}_5)_2]$ consisting of two bridged bidentate benzoate moieties bound to the copper(II) ions. The rearrangement of

chemical bonds causes change, in the geometry to more distorted square pyramidal ($\tau = 28\%$) and copper(II) ion coordination environment from CuNO_4 (**2**) to CuN_2O_3 , by increasing the nitrogen donor connecting sites. In dimeric unit, each copper center is coordinated by two imidazolyl nitrogen atoms from two distinct thim_2 ligands [Cu–N lengths of 2.003(4) Å and 2.007(4) Å] and three oxygen atoms, one from mono-dentate (Cu1–O3=1.979(4) Å) coordinated benzoate and remaining two from bridged bidentate benzoates. One oxygen atom of bridged bidentate benzoates occupy the position at the square plane (Cu1–O2=1.957(4) Å) whereas the other oxygen atom coordinates at the axial position [Cu1–O1 length of 2.311(4) Å] (Figure 4a). The Cu–N/O bond distances are found to be consistent with the reported copper containing CPs.^{29, 48} Within the dimeric unit, the oxygen atoms of the bridged bidentate benzoate units are bound to the copper ion in *syn-anti* connecting mode. As compared to **2**, in **3** Cu–Cu distance in the dimeric unit is increased to 4.404 Å whereas the dihedral angle between the imidazolyl rings in thim_2 is decreased (14.39°). The imidazolyl nitrogen atoms of thim_2 connect the dimeric units, leading to the formation of a 1D ladder type chain structure (Figure 4b). These 1D chains are further connected to form a 3D supramolecular structure through C–H \cdots O (along a direction) and C–H $\cdots\pi$ interactions (in bc plane) (Figure 4c; S3a-b). In **3**, the intra- (12.95 Å) and inter-chain Cu–Cu distances (11.75 Å and 9.93 Å) are differed significantly from **2**.

Structural analysis of $\{[\text{Cu}_2(\text{thim}_2)_2(\mu_2\text{-OH}_2)(\text{OOC}_6\text{H}_5)_4]\cdot 4\text{H}_2\text{O}\}_n$ (**4**)

In order to ascertain the stability of **3**, mother solution containing these crystals was left for about 20 days under air. Surprisingly blue colored crystals changed into dark blue colored crystals of **4** and confirm CP **3** as a intermediate kinetic product in the process of formation of thermodynamically stable CP **4**. The X-ray structural analysis of **4** shows that bridging mode of benzoate in the dimeric unit $[\text{Cu}_2(\text{OOC}_6\text{H}_5)_2]$ of **3** is destroyed and simultaneous chemical

rearrangement transform the structure into a 2D network. It consists of two distorted square pyramidal ($\tau = 6^\circ$) copper(II) ions bridged by the water molecule axially. Each Cu(II) ion is coordinated by two nitrogen atoms of imidazole units from two different thim_2 and two oxygen atoms from two monodentate benzoate groups at the square plane (Figure 5a). Interestingly, the square planes in these two copper centers are oriented with the dihedral angle of 31.77° which is responsible for generating a 2D network (Figure 5b). The thim_2 ligand connects the two metal centers (Cu1 and Cu2), form a 1D chain. In the network, each copper- thim_2 chains are helical in nature and consist of opposite helicity in the adjacent chains. The two helical chains propagate in almost perpendicular directions like 1O/1U to form a 2D plain weave like pattern (Figure S4a). All the Cu–N/O bond distances are found consistent with other similar CPs, however the Cu–O distance involving the H_2O molecule is found be longer [Cu1–Ow = 2.399(5) Å and Cu2–Ow = 2.330(5) Å] than the $\{[\text{Cu}(\text{OAc})_2(\text{Phen})]_2\mu\text{-H}_2\text{O}\}$.⁴⁹ The Cu–Cu distance in **4** between the copper centers is 4.60 Å which is slightly longer than **3**. Also, the intra-chain Cu \cdots Cu separation is 12.70 Å and 12.58 Å. Two thim_2 ligands are present in asymmetric unit and dihedral angle between two imidazole rings are $33.47(8)^\circ$ and $42.34(1)^\circ$ respectively. These 2D layers are arranged in $\cdots ABAB \cdots$ fashion through C–H \cdots O and $\pi\cdots\pi$ interactions and stacking of all layers generates a 3D array (Figure 5c; S4b).

Role of the ligand and supramolecular interactions in SC-SC Transformation

The SC-SC transformation from **2** to **3** with visible changes from green to blue crystals upon exposing the mother solution to air was indeed surprising. This shows that presence of air and excess of ligand in the solution play important role in transformation. Careful analysis of the structure **2** reveals some of the important information's related to **2** which could be responsible for its stability and also for the kinetically driven SC-SC transformations. There are supra-

molecular interactions such as C–H \cdots O, C–H \cdots π , and $\pi\cdots\pi$ are present in 3D structure. In two adjacent inter-chains, C–H \cdots O interactions between the backbone C–H of thiophene (C6–H6)/imidazole(C3–H3) groups and the oxygen atoms (O3 and O7) of carboxylate units and short perpendicular interactions between imidazole (C1) and (C14, C15 and C16) carbon atoms of phenyl ring are present (Figure S2b). These interactions are present at the cost of angle strain between the imidazole units of thim_2 which generate the non-planar connectivity between the two paddle wheel units. In addition, closer distance between Cu1 and Cu2 of adjacent chain's paddle wheel units was found to be 7.49 Å (Figure S2b). Thus in **2**, the overall arrangement of atoms are present in constrained environment which might causes the lattice strain and make CP **2** as kinetic product which transform to more kinetically stable CP **3** under air using the remaining thim_2 present in solution. During this transformation, we did not observed dissolution of the crystals in solution and X-ray data measurements of random crystals after 12 h, indicating a spontaneous SC-SC transformation. The bulk sample purity of CPs **2** and **3** was also confirmed through PXRD (Figure S9-10). The structure of CP **3** show more ordered arrangement with reduced dihedral angle between the imidazole units of thim_2 and the lesser number of supramolecular interactions which indicate the release of above mentioned strain. However, in this case the geometry around the copper (II) ions is distorted as compared to **2**. Thus leaving the crystals of **3** in mother solution under air for about 20 days resulted in the formation of even more stable 2D network of CP **4** in SC-SC manner. In CP **4**, the square pyramidal geometry ($\tau = 6^\circ$) of copper (II) ions is less distorted as compared to CP **3** and imidazole units of thim_2 attain the intermediate [33.47(8) $^\circ$ and 42.34 (1) $^\circ$] dihedral angle. These changes indicate the complete release of geometrical strain and the formation of a thermodynamic product **4**. In the whole transformation series from **2** to **4** air played an crucial role. Such examples were reported

previously in the literature. Unfortunately, the transformation of **3** to **4** was not reproducible even after several attempts.

Magnetic detail of CPs 1-3

Inspired by the structural changes at the room temperature, the corresponding change in magnetic properties was envisaged. Thus the temperature dependent magnetic measurements ($\chi_m T$ versus T plots) for CPs **1-3** are shown in the Figure 6a. A gradual decrease in the $\chi_m T$ with the temperature for CPs **1** and **2** reveal dominant antiferromagnetic interaction between the neighbouring Cu(II) centers. As compared to that, $\chi_m T$ values for **3** increases gradually as the temperature increases indicating dominant ferromagnetic behaviour. Decrease in $\chi_m T$ values below 20K can be attributed to intermolecular interactions or zero-field splitting.

For CP **1**, a gradual decrease in $\chi_m T$ is observed with the decrease in temperature suggesting deviation from Curie behaviour. This indicates weak to moderate antiferromagnetic interaction between two Cu(II) centers despite long Cu...Cu distances observed (Figure 6a). While in CP **2** the magnetic behaviour is dominated by paddle wheel Cu(II) benzoates interaction. Such interactions are known to extremely antiferromagnetic, thus the magnetic properties and sharp decline in the $\chi_m T$ are characteristics of the $\{\text{Cu}_2(\text{OAC})_4\}$ moiety.⁵⁰ For CP **3**, interestingly increase in the $\chi_m T$ with temperatures observed. Here the Cu(II) centers are sitting in different plane leading to parallel Jahn-Teller elongation and likely orthogonality between the $d_{x^2-y^2}$ orbitals leads to ferromagnetic coupling. A weak to moderate ferromagnetic coupling can be expected here (Figure 6b).⁵¹

TG analysis and PXRD

TG analysis is carried out to examine the thermal stability of CPs **1-3** under nitrogen atmosphere (Figure S5-7). For CP **1** thermal stability was observed upto 200 °C beyond that

compound decompose rapidly. CP **2** exhibits the stability upto 230 °C and above this CP start to decompose. TGA plot shows CP **3** is stable upto 210 °C and beyond this temperature decomposition of the compound starts. PXRD spectra of CPs (**1-3**) indicate the experimental pattern was consistent with the simulated pattern which confirms the phase purity of all the compounds (Figure S8-10).

Conclusion

In conclusion, we have synthesized three 1D (**1-3**) and one 2D (**4**) CPs. CPs (**2-4**) were obtained through irreversible and sequential SC-SC transformations. The transformation of **2-4** is associated with breaking of $[\text{Cu}_2(\text{OOCCH}_2\text{C}_6\text{H}_5)_4]$ paddle wheel unit (**2**) and formation of a new $[\text{Cu}_2(\text{OOCCH}_2\text{C}_6\text{H}_5)_2]$ dimeric unit (**3**) which subsequently form a water bridged copper dimeric unit (**4**). In **2-4** square pyramidal geometry of copper ion is retained. Moreover, connecting modes of benzoate anions to the copper centers as well as dihedral angle between imidazole units in thim_2 play an important role in the formation of different structures. The transformation may be caused by the lattice instability in **2** and **3** due to the strain induced by the ligand orientations which suggest that **2** and **3** are kinetic products before forming a thermodynamically stable product **4**. The change in the structures reflects the difference in magnetic behavior of **2** and **3**.

ASSOCIATED CONTENT

SUPPORTING INFORMATION

Additional figures, TGA, PXRD. X-ray crystallographic data in CIF format have been deposited with the Cambridge Structural Database (CCDC 911877, 945262, 925605, 945263).

AUTHOR INFORMATION

Corresponding author

*^a E-mail: garaman@iitk.ac.in

ACKNOWLEDGMENTS

The authors thank the Council of Scientific and Industrial Research (CSIR), and Department of Science and technology (DST), Government of India for their financial support and the Indian Institute of Technology (IIT), Kanpur for infrastructural facilities. NS thank University Grant Commission (UGC) for providing fellowship to do doctoral study. We are immensely grateful to Professor Ratnamala Chatterjee for the help and suggestions in collecting magnetic data and Professor Gopalan Rajaraman for the help in analysing magnetic data.

References:

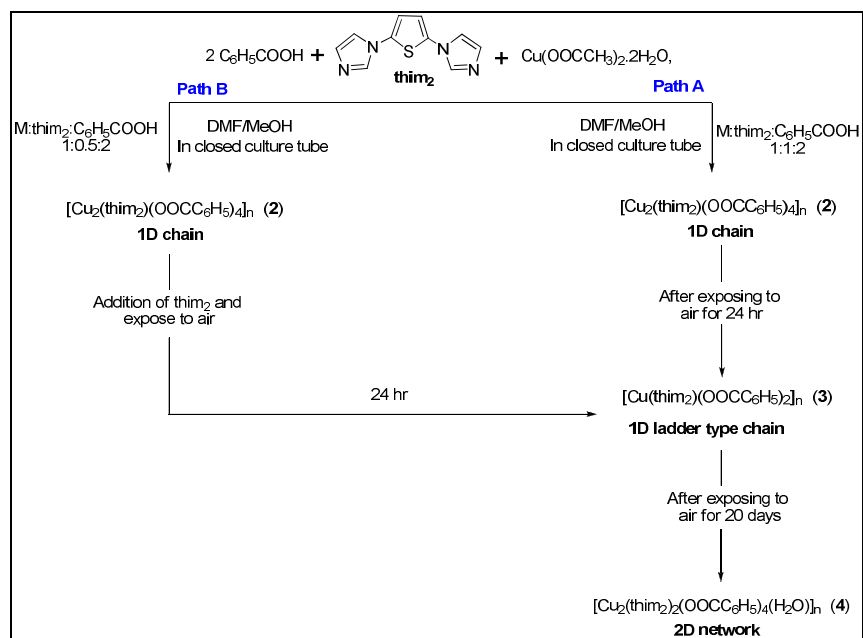
1. Y. Yan, S. Yang, A. J. Blake and M. Schröder, *Acc. Chem. Res.*, 2014, **47**, 296.
2. M. Kurmoo, *Chem. Soc. Rev.*, 2009, **38**, 1353.
3. D. Farrusseng, S. Aguado and C. Pinel, *Angew. Chem. Int. Ed.*, 2009, **45**, 7502.
4. J.-P. Zhang, P.-Q. Liao, H.-L. Zhou, R.-B. Lin and X.-M. Chen, *Chem. Soc. Rev.*, 2014, **43**, 5789.
5. G. K. Kole and J. J. Vittal, *Chem. Soc. Rev.*, 2013, **42**, 1755.
6. W. L. Leong and J. J. Vittal, *Chem. Rev.*, 2010, **111**, 688.
7. A. Chanthapally, W. T. Oh and J. J. Vittal, *Chem. Commun.*, 2014, **50**, 451.
8. M. Oh, L. Rajput, D. Kim, D. Moon and M. S. Lah, *Inorg. Chem.*, 2013, **52**, 3891.
9. A. M. P. Peedikakkal and J. J. Vittal, *Cryst. Growth Des.*, 2011, **11**, 4697.
10. S. Y. Lee, J. H. Jung, J. J. Vittal and S. S. Lee, *Cryst. Growth Des.*, 2010, **10**, 1033.
11. S. Mishra, E. Jeanneau, H. Chermette, S. Daniele and L. G. Hubert-Pfalzgraf, *Dalton Trans.*, 2008, 620.
12. X. Wang and J. J. Vittal, *Inorg. Chem.*, 2003, **42**, 5135.
13. M. Kawano and M. Fujita, *Coord. Chem. Rev.*, 2007, **251**, 2592.
14. Y.-H. Liu, S.-H. Lee, J.-C. Chiang, P.-C. Chen, P.-H. Chien and C.-I. Yang, *Dalton Trans.*, 2013, **42**, 16857.
15. J. J. Vittal, *Coord. Chem. Rev.*, 2007, **251**, 1781.
16. S. Kitagawa and R. Matsuda, *Coord. Chem. Rev.*, 2007, **251**, 2490.
17. M. Du, C.-P. Li, C.-S. Liu and S.-M. Fang, *Coord. Chem. Rev.*, 2013, **257**, 1282.

18. A. Schneemann, V. Bon, I. Schwedler, I. Senkovska, S. Kaskel and R. A. Fischer, *Chem. Soc. Rev.*, 2014, **43**, 6062.
19. J. Seo, C. Bonneau, R. Matsuda, M. Takata and S. Kitagawa, *J. Am. Chem. Soc.*, 2011, **133**, 9005.
20. D. N. Dybtsev, H. Chun and K. Kim, *Angew. Chem. Int. Ed.*, 2004, **43**, 5033.
21. A. B. Lago, R. Carballo, S. Rodríguez-Hermida and E. M. Vázquez-López, *Cryst. Growth Des.*, 2014, **14**, 3096.
22. Y.-Q. Lan, H.-L. Jiang, S.-L. Li and Q. Xu, *Inorg. Chem.*, 2012, **51**, 7484.
23. M. Du, C.-P. Li, J.-M. Wu, J.-H. Guo and G.-C. Wang, *Chem. Commun.*, 2011, **47**, 8088.
24. X.-D. Chen, X.-H. Zhao, M. Chen and M. Du, *Chem. Eur. J.*, 2009, **15**, 12974.
25. C. Hou, J.-M. Shi, Y.-M. Sun, W. Shi, P. Cheng and L.-D. Liu, *Dalton Trans.*, 2008, 5970.
26. Y. Reyes-Ortega, J. L. Alcántara-Flores, M. C. Hernández-Galindo, D. Ramírez-Rosales, S. Bernès, J. C. Ramírez-García, R. Zamorano-Ulloa and R. Escudero, *J. Am. Chem. Soc.*, 2005, **127**, 16312.
27. S. Shova, G. Novitchi, M. Gdaniec, A. Caneschi, D. Gatteschi, L. Korobchenko, Violeta K. Voronkova, Yurii A. Simonov and C. Turta, *Eur. J. Inorg. Chem.*, 2002, **2002**, 3313.
28. R. Sarma, A. K. Boudalis and J. B. Baruah, *Inorg. Chimica Acta*, 2010, **363**, 2279.
29. C.-S. Liu, J.-J. Wang, L.-F. Yan, Z. Chang, X.-H. Bu, E. C. Sañudo and J. Ribas, *Inorg. Chem.*, 2007, **46**, 6299.
30. F. Nouar, J. F. Eubank, T. Bousquet, L. Wojtas, M. J. Zaworotko and M. Eddaoudi, *J. Am. Chem. Soc.*, 2008, **130**, 1833.
31. R.-Q. Zou, H. Sakurai, S. Han, R.-Q. Zhong and Q. Xu, *J. Am. Chem. Soc.*, 2007, **129**, 8402.
32. B. Schmidt, J. Jiricek, A. Titz, G. Ye and K. Parang, *Bioorg. Med. Chem. Lett*, 2004, **14**, 4203.
33. S. A. Bourne, J. Lu, A. Mondal, B. Moulton and M. J. Zaworotko, *Angew. Chem. Int. Ed.*, 2001, **40**, 2111.
34. S. S.-Y. Chui, S. M.-F. Lo, J. P. H. Charmant, A. G. Orpen and I. D. Williams, *Science*, 1999, **283**, 1148.

35. F. P. W. Agterberg, H. A. J. Provó Kluit, W. L. Driessen, H. Oevering, W. Buijs, M. T. Lakin, A. L. Spek and J. Reedijk, *Inorg. Chem.*, 1997, **36**, 4321.
36. N. Singh and G. Anantharaman, *CrystEngComm*, 2014, **16**, 7914.
37. N. Singh and G. Anantharaman, *CrystEngComm*, 2014, **16**, 6203.
38. B. S. Furniss, A. J. Hannaford, P. W. G. Smith and A. R. Tatchell, *Pearson Education, Longman Group UK, 5th edn.*, 2005.
39. E. König, 1966.
40. A. C. Altomare, G.; Giacovazzo, C.; Guagliardi, A., *J. Appl. Crystallogr.*, 1993, **26**, 343–450.
41. G. M. Sheldrick, *SHELXL-97, Program for Crystal Structure Solution and Refinement, University of Göttingen, Göttingen, Germany*, 1997.
42. G. M. Sheldrick, *Acta Crystallogr.* , 2008, **A64**, 112–122.
43. A. L. P. Spek, *Acta Cryst.*, 2009, **D65**, 148-155.
44. K. Nakamota, *Wiley, New York*, 1986.
45. G. B. Deacon and R. J. Phillips, *Coord. Chem. Rev.*, 1980, 227.
46. H.-X. Zhao, G.-L. Zhuang, S.-T. Wu, L.-S. Long, H.-Y. Guo, Z.-G. Ye, R.-B. Huang and L.-S. Zheng, *Chem. Commun.*, 2009, 1644.
47. S. Takamizawa, E.-i. Nakata and T. Saito, *Inorg. Chem. Commun.*, 2004, **7**, 1.
48. S. Tanase, G. A. van Albada, R. de Gelder, E. Bouwman and J. Reedijk, *Polyhedron*, 2005, **24**, 979.
49. M. Barquín, M. J. G. Garmendia, L. Larrínaga, E. Pinilla and M. R. Torres, *Z. Anorg. Allg. Chem.*, 2005, **631**, 2151.
50. B. Bleaney and K. D. Bowers, *Proc. Roy. Soc. London A 214*,, 1952, 451–465.
51. O. Kahn, *Molecular Magnetism, VCH Publishers, Inc., New York, USA* , 1993.

Table 1. Crystal data and structure refinement parameters for CPs 1-4

Compound	1	2	3	4
Empirical formula	C ₁₄ H ₁₄ N ₄ O ₄ SCu	C ₃₈ H ₂₈ N ₄ O ₈ SCu ₂	C ₂₄ H ₁₈ N ₄ O ₄ SCu	C ₄₈ H ₄₄ N ₈ O ₁₃ S ₂ Cu ₂
Formula wt.	397.89	827.78	522.02	1132.11
Crystal System.	Monoclinic	Triclinic	Triclinic	Monoclinic
Space group	<i>P</i> 2 ₁ / <i>n</i>	<i>P</i> -1	<i>P</i> -1	<i>P</i> 2 ₁ / <i>c</i>
<i>a</i> (Å)	9.671(2)	10.070(5)	9.927(5)	16.724(3)
<i>b</i> (Å)	16.721(3)	10.681(6)	9.945(5)	15.975(3)
<i>c</i> (Å)	9.760(2)	18.871(12)	11.752(5)	18.456(4)
α , deg	90	85.22(2)	92.242(5)	90
β , deg	94.855(4)	74.62(2)	104.517(5)	91.46(3)
γ , deg	90	71.56(2)	98.603(5)	90
<i>V</i> /Å ³	1572.6(6)	1856.5(18)	1103.0(9)	4929(17)
<i>Z</i>	4	2	2	4
$\rho_{\text{calc.}}$ g/cm ³	1.681	1.481	1.572	1.526
μ , mm ⁻¹	1.549	1.259	1.126	1.021
<i>F</i> (000)	812	844	534	2328
Reflns collected	9297	13947	6702	25221
Indep. Reflns	3414	6467	4670	9678
GOF	1.056	1.187	1.057	0.871
<i>R</i> ₁ / <i>wR</i> ₂ [<i>I</i> > 2 σ (<i>I</i>)]	0.0535, 0.1265	0.0948, 0.1834	0.0574, 0.1414	0.0734, 0.1926
<i>R</i> ₁ / <i>wR</i> ₂ (all data)	0.0854, 0.1625	0.1053, 0.1894	0.0856, 0.1978	0.1611, 0.2280



Scheme 1. Structural transformation from 2 to 4

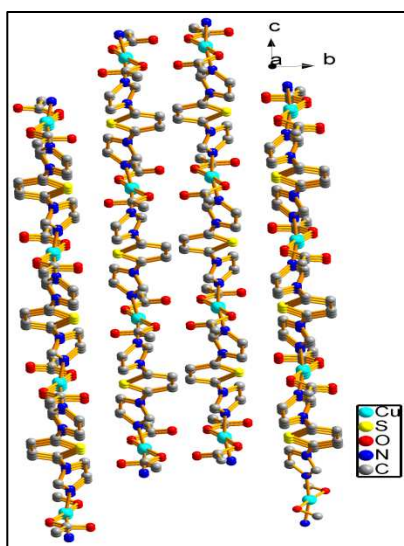
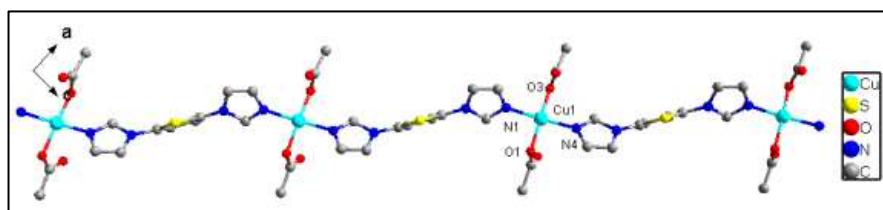
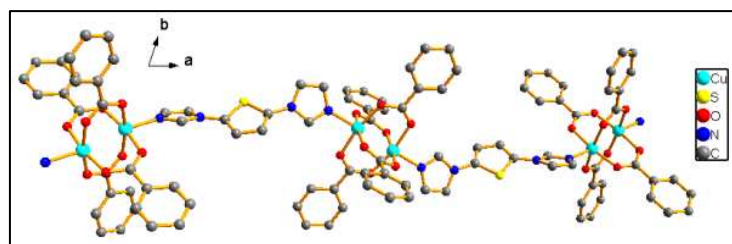
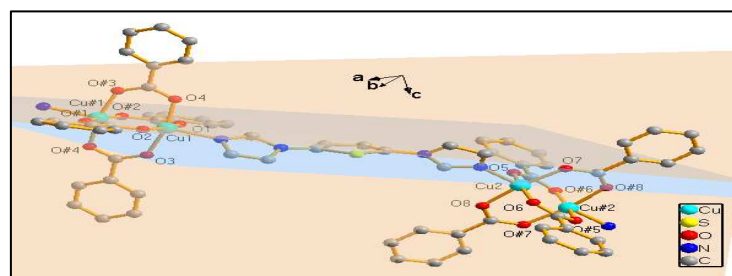


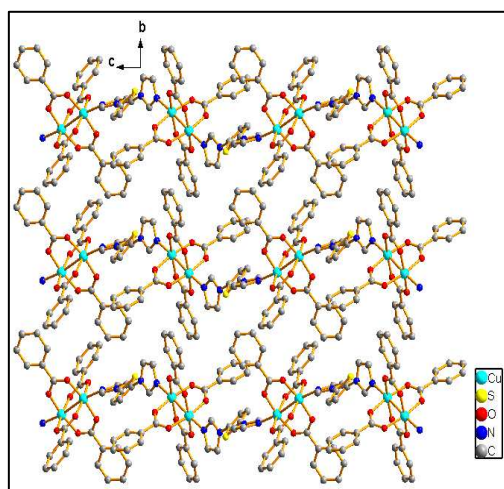
Figure 1. (a) 1D polymer chain of 1 (b) 3D supramolecular packing of CP 1



(a)



(b)



(c)

Figure 2. (a) 1D polymer chain of **2** (b) Coordination environment around Cu1(II) and Cu2(II) ion and plane between eight member rings (c) 3D supramolecular packing of CP **2**

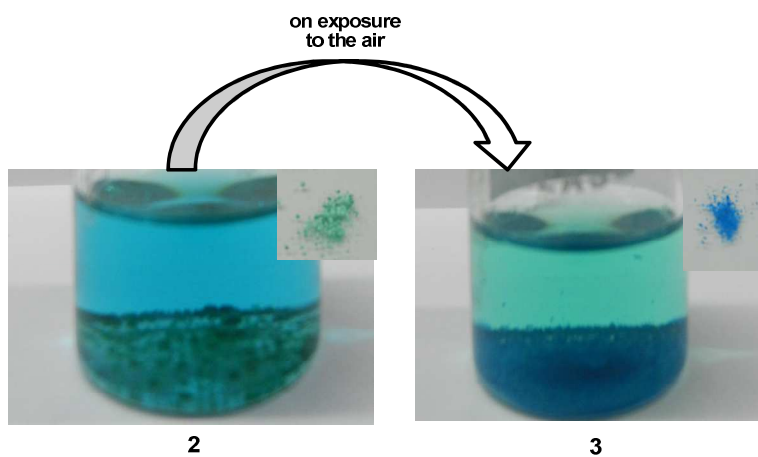


Figure 3 Transformation of green crystals of **2** to blue crystals of **3**

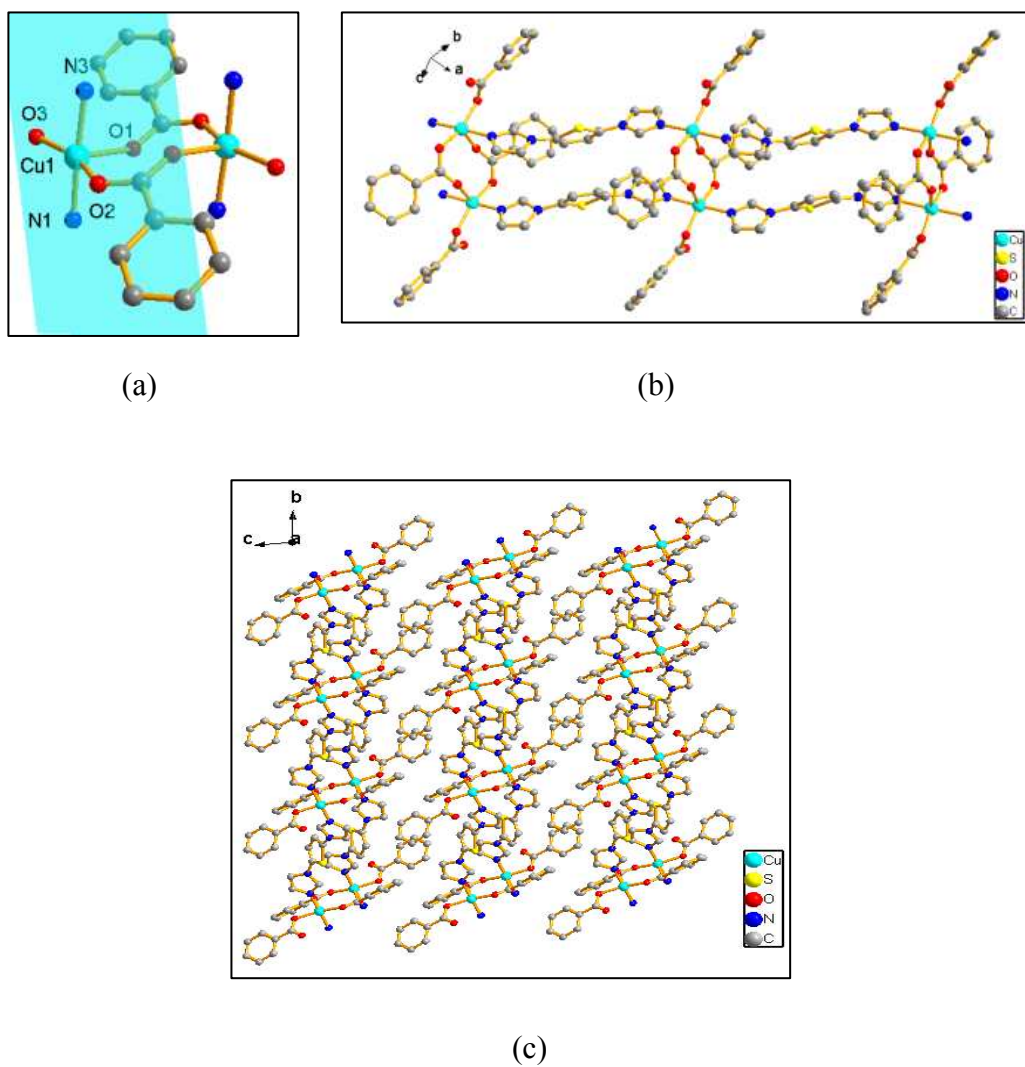
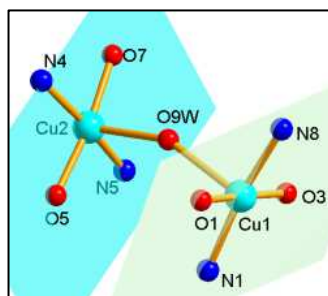
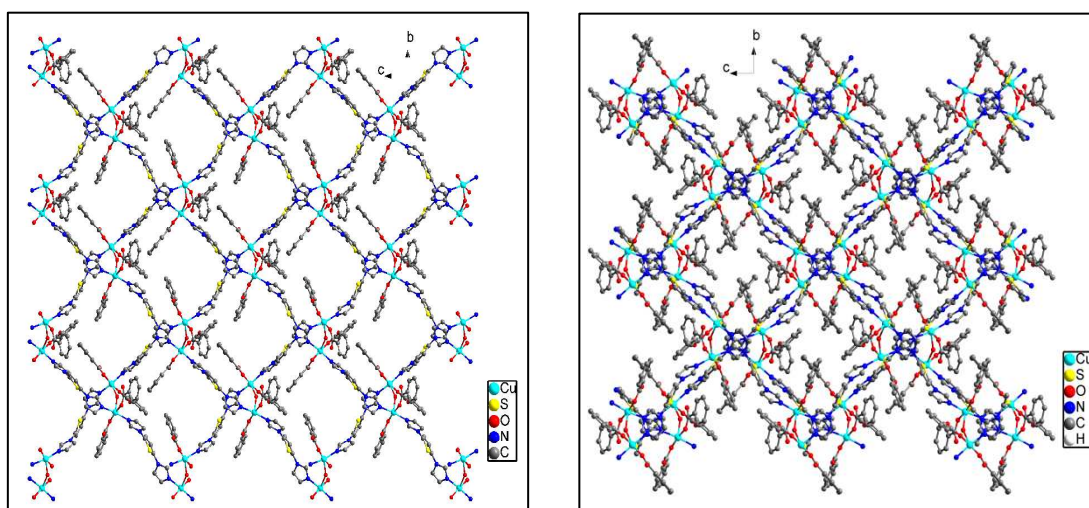


Figure 4. (a) Coordination environment around Cu(II) in **3** with square plane (b) 1D ladder type chain (c) 3D supramolecular packing of CP **3**



(a)



(b)

(c)

Figure 5. (a) Coordination environment surrounding Cu1(II) and Cu2(II) ion in **4** with square plane (b) 2D network along the crystallographic *bc* plane (c) Three dimensional packing of **4** along the *a* axis

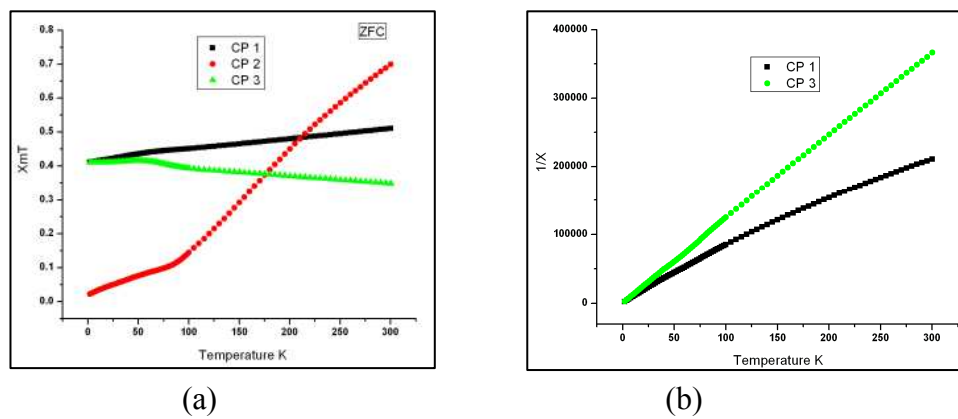


Figure 6. (a) $\chi_m T$ product for CPs **1-3** as a function of temperature (b) $1/\chi$ product for CPs **1** and **3** as a function of temperature

For the Table of Contents only

Coordination Polymers Based on Copper Carboxylates and Angular 2,5-bis(imidazol-1-yl)thiophene (thim₂) Ligand: Sequential Structural Transformations

Namita Singh^a, Pratap Vishnoi^b and Ganapathi Anantharaman^{*a}

^a*Department of Chemistry, Indian Institute of Technology (IIT), Kanpur – 208016, India.*

^b*Department of Chemistry, Indian Institute of Technology (IIT), Bombay, Powai, Mumbai –
400076, India.*

Email: garaman@iitk.ac.in.

A 1D helical chain (**1**) and one pot sequential transformation of 1D zigzag (**2**) chain into 1D ladder type chain (**3**) and further into 2D network (**4**) have been reported. Magnetic behaviour for CPs **1-3** have been investigated.

